Supplement of Geosci. Model Dev., 19, 1103–1120, 2026
https://doi.org/10.5194/gmd-19-1103-2026-supplement

Geoscientific Model Development
Open Access

Supplement of

LEX v1.6.0: a new large-eddy simulation model in JAX with GPU acceleration and automatic differentiation

Xingyu Zhu et al.

Correspondence to: Xiaoming Shi (shixm@ust.hk)

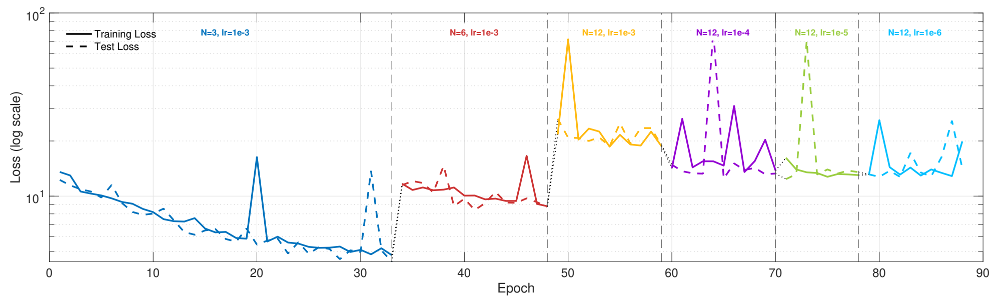

Figure S1. The loss record for the training and testing of the hybrid model.

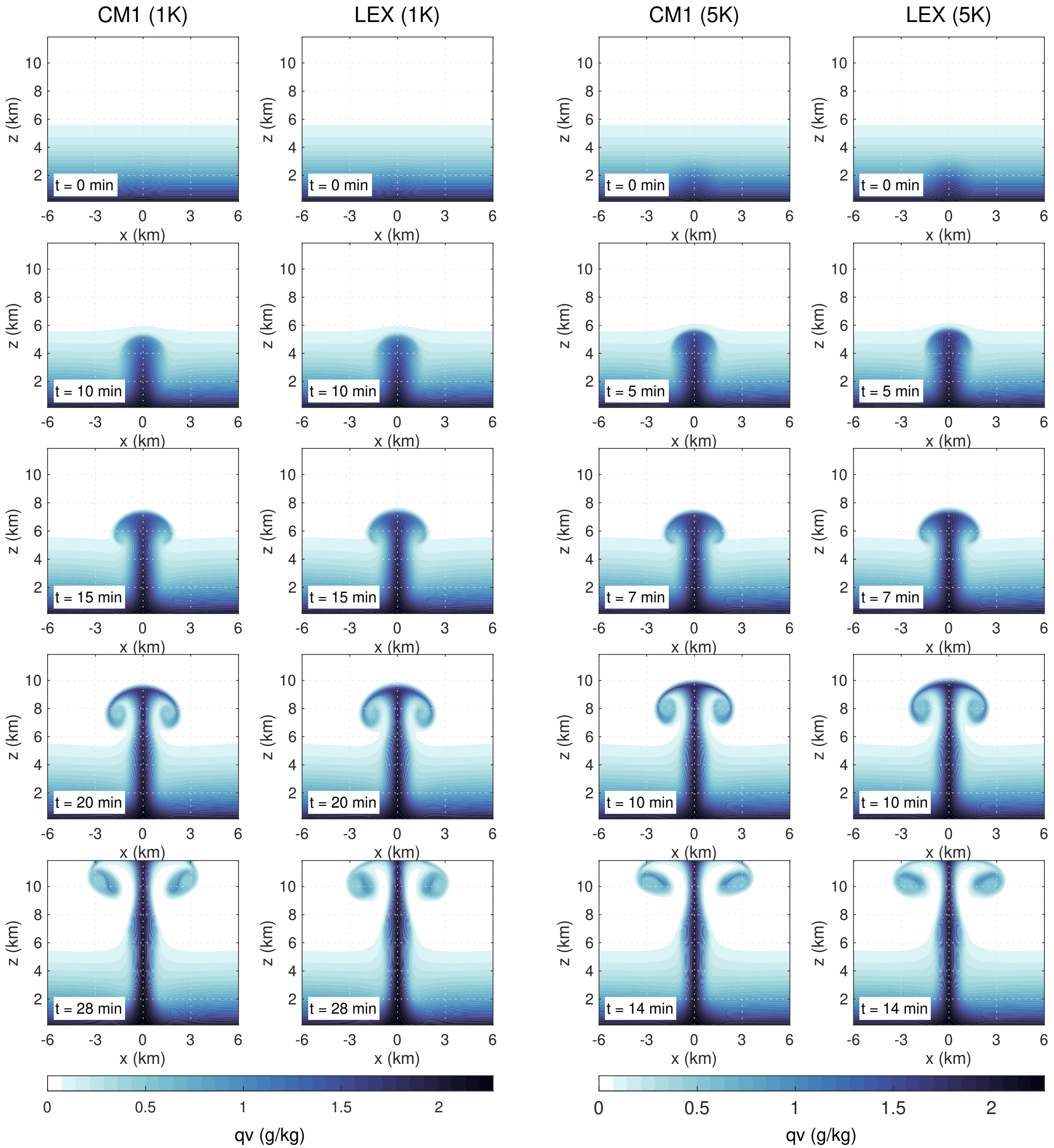

Figure S2. Snapshots of simulated mixing ratio of water vapor (q_v) in CM1 and LEX under different initial central potential temperature perturbations: 1 K at t = 0, 10, 15, 20, and 28 min (the first and second columns) and 5 K at t = 0, 5, 7, 10, and 14 min (the third and fourth columns).

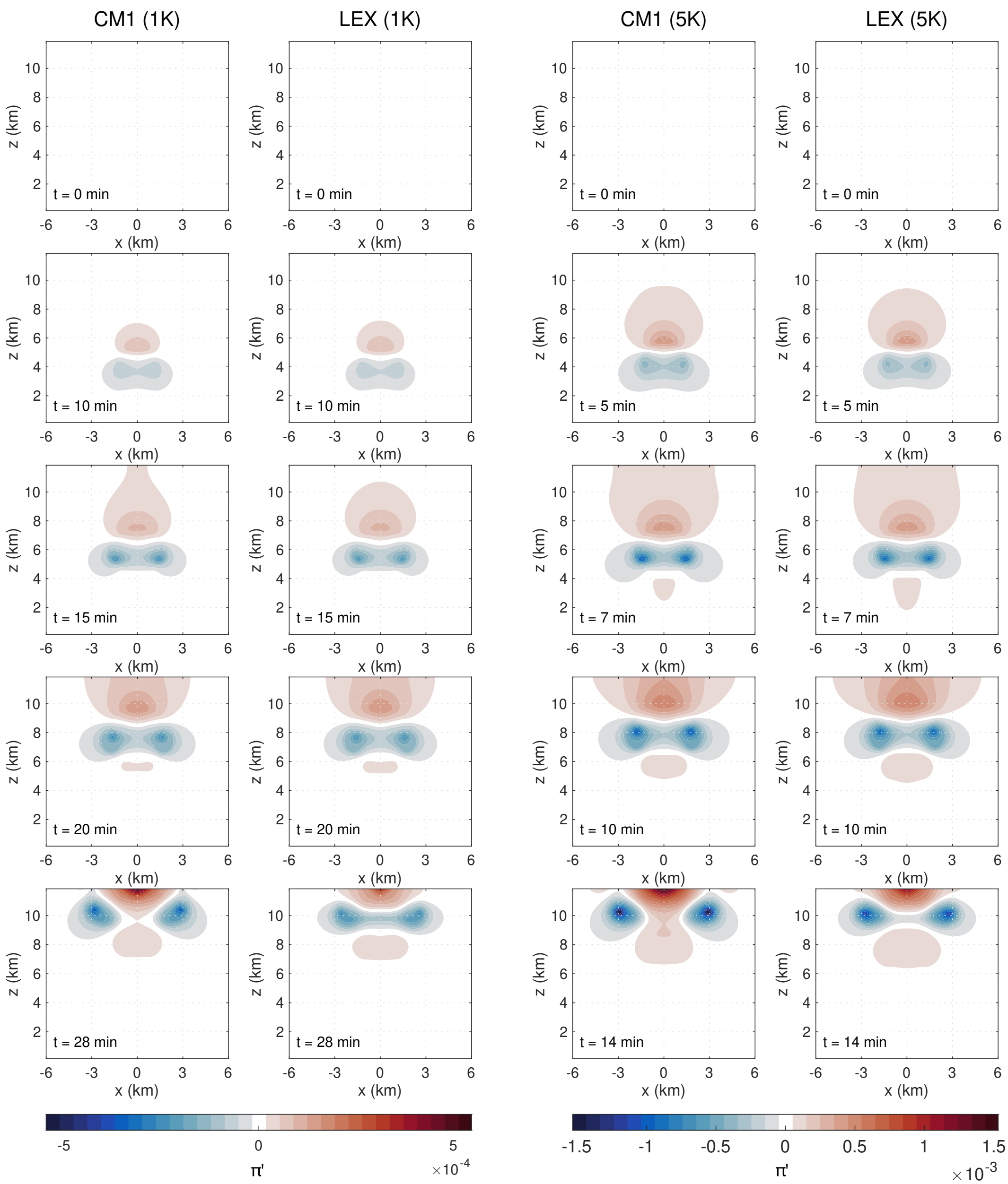

Figure S3. Snapshots of simulated pressure perturbations (π') in CM1 and LEX under different initial central potential temperature perturbations: 1 K at t = 0, 10, 15, 20, and 28 min (the first and second columns) and 5 K at t = 0, 5, 7, 10, and 14 min (the third and fourth columns).

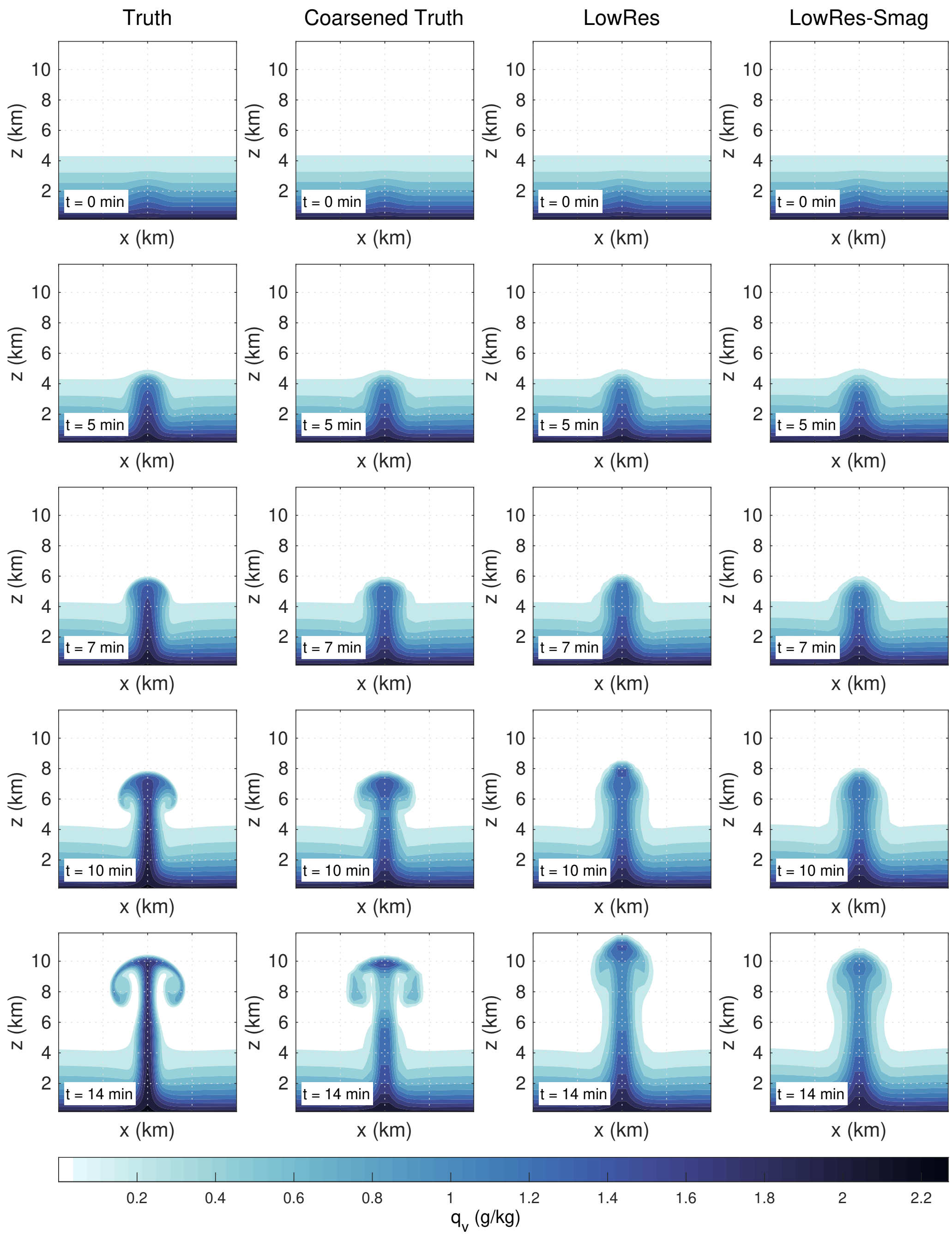

Figure S4. Snapshots of simulated water vapor mixing ratio (q_v) at t = 0, 5, 7, 10, and 14 min, with $\theta_c = 5K$, where the first column is the 'Truth' simulation with a high resolution of $100 \times 100 \times 100m$, the second column is coarsen-grained from the Truth simulation with a coarse resolution of $600 \times 600 \times 300m$, the third column is the numerical simulation results with the coarse grids, and the forth column is the LowRes simulation with the Smargorinsky scheme to deal with the SGS turbulence.

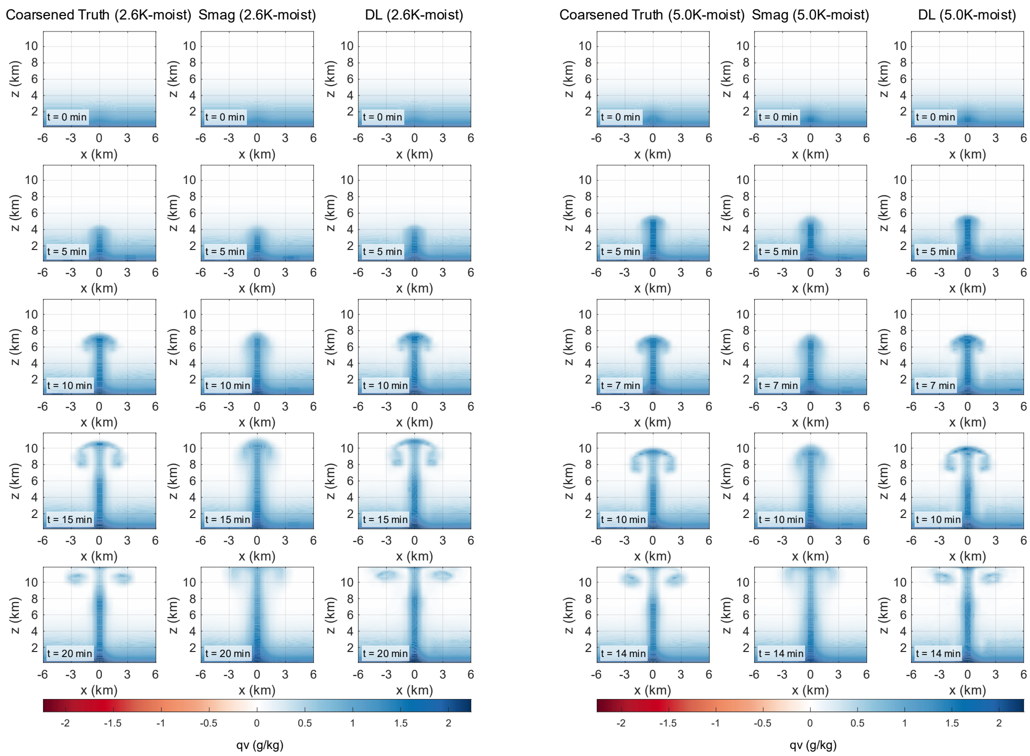

Figure S5. Snapshots of simulated water vapor mixing ratio (q_v) at t = 0, 5, 10, 15, and 20 min for moist cases, with $\theta_c = 2.6K$ (the first to the third columns), and $\theta_c = 5.0K$ (the fourth to the sixth columns), where the first and fourth columns are the 'Coarsened Truth' simulations with a coarse resolution of $600 \times 600 \times 300m$, the second and fifth columns are the 'LowRes-Smag' simulations with the Smagorinsky scheme to deal with the SGS turbulence, and the third and sixth columns are 'LowRes-DL' simulations with the trained AE model to serve as the turbulence parameterization scheme.

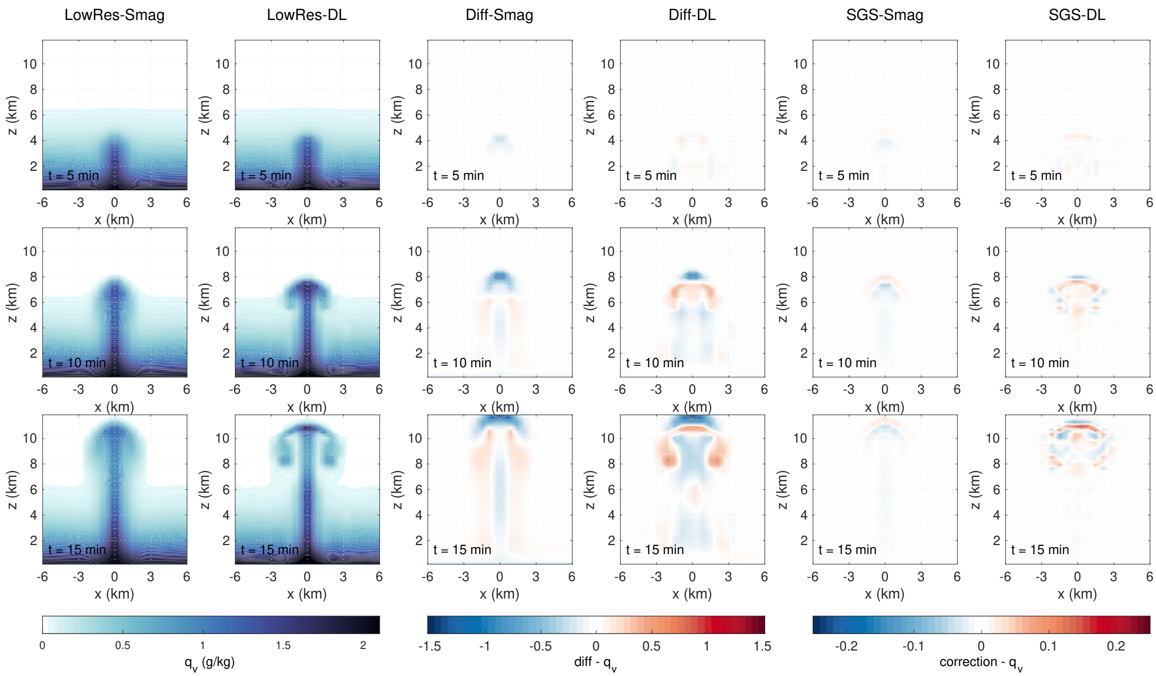

Figure S6. The simulated water vapor mixing ratio (q_v) at t = 5, 10, and 15 min, with $\theta_c = 2.6K$. The first and second columns are the forecasts of the conventional Smagorinsky and DL-based SGS model. The third and fourth columns are the differences between parameterized and non-parameterized simulation results of the conventional Smagorinsky and the DL-based SGS model. The fifth column is the SGS tendency due to the Smagorinsky model, and the sixth column is the SGS correction due to the DL model.

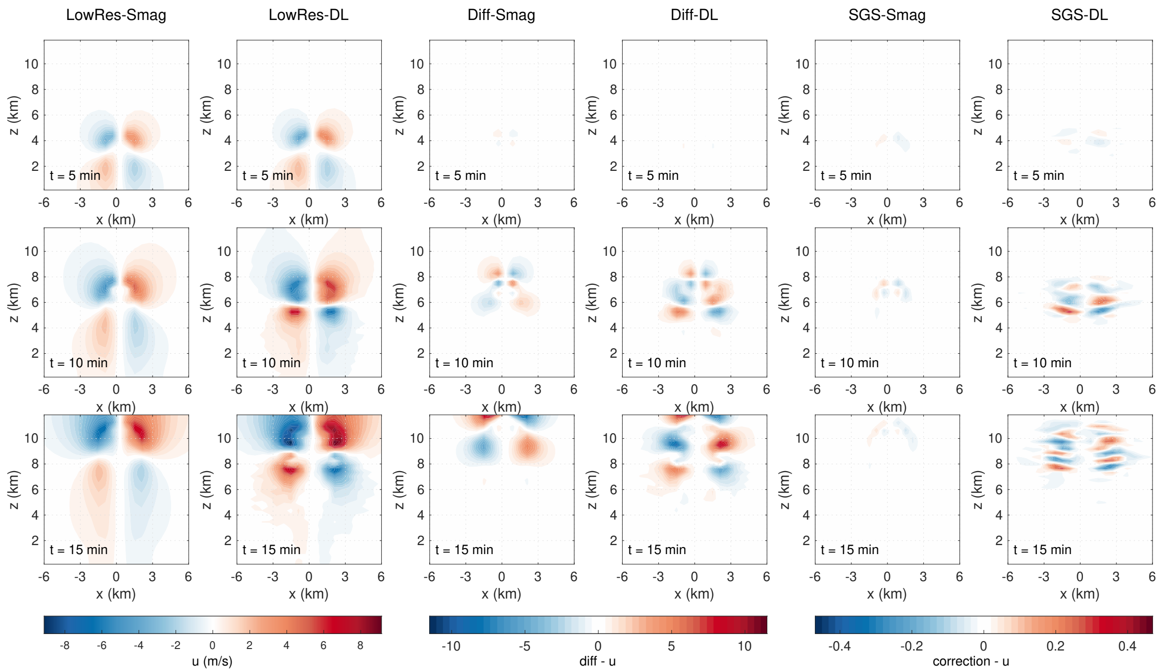

Figure S7. The simulated horizontal wind (u) at t = 5, 10, and 15 min, with $\theta_c = 2.6K$. The first and second columns are the forecasts of the conventional Smagorinsky and DL-based SGS model. The third and fourth columns are the differences between parameterized and non-parameterized simulation results of the conventional Smagorinsky and the DL-based SGS model. The fifth column is the SGS tendency due to the Smagorinsky model, and the sixth column is the SGS correction due to the DL model.

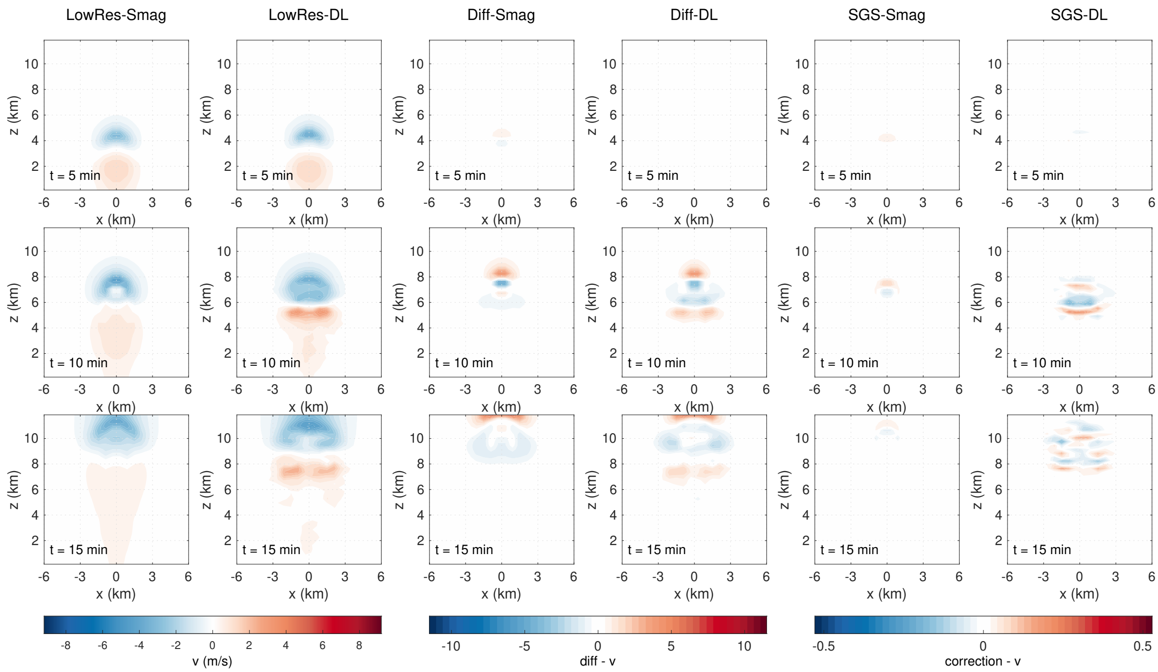

Figure S8. The simulated horizontal wind (v) at t = 5, 10, and 15 min, with $\theta_c = 2.6K$. The first and second columns are the forecasts of the conventional Smagorinsky and DL-based SGS model. The third and fourth columns are the differences between parameterized and non-parameterized simulation results of the conventional Smagorinsky and the DL-based SGS model. The fifth column is the SGS tendency due to the Smagorinsky model, and the sixth column is the SGS correction due to the DL model.